

Interplay of Structural, Magnetic and Superconducting Properties in the Compounds CeCoIn₅ and CeIrIn₅

Steffen Wirth, Andrea D. Bianchi¹, Horst Borrmann, Stefan Ernst, Zachary Fisk², Sunil Nair³, Michael Nicklas, Oliver Stockert, Yuri Prots, Reiner Ramlau, John L. Sarrao⁴, Joe D. Thompson⁴, Ulrike Witte⁵, Yuri Grin, and Frank Steglich

Heavy-fermion metals typically contain 4*f* or 5*f* elements (*e.g.* Ce, Yb or U) and are characterized by a dramatic increase of the effective mass of the charge carriers at low temperatures which may reach up to several hundred times the mass of a free electron. This is brought about by a magnetic interaction – the so-called Kondo effect – which couples the free electrons to the local *f* magnetic moments (and hence, to those electrons that are fixed to the crystal lattice) such that the latter magnetic moments are effectively screened. The properties of these metals can often be described, according to Landau, by considering quasi-particles made up of the electrons and their interactions instead of the mere electrons within the free electron gas. In addition, in many of these materials an indirect exchange coupling between the local magnetic moments is found (the so-called RKKY interaction) which is also mediated – just like the aforementioned Kondo interaction – via the conduction electrons. Hence, these two interactions are in direct competition. The relative strength of these two competing interactions can be tuned by experimental parameters such as chemical doping, pressure and magnetic field. In case of this competition being adequately balanced a quantum phase transition (QPT) at $T = 0$ can be brought about by a well-directed change of these experimental parameters [1].

With the Kondo and RKKY ground states well balanced additional, smaller energy scales may play a decisive role. In fact, in many cases superconductivity is observed in close proximity to a quantum critical point (QCP), *i.e.* the point in phase space at which a *continuous* QPT occurs [2]. Possibly, superconductivity is one way of disposing the huge entropy accumulated in the vicinity of a QCP. This concept has been generalized [3] such that possibly even in the copper-oxide materials superconductivity might be related to a hidden QCP. In this context it should be noted that superconductivity for which such a scenario is discussed is commonly considered to be of unconventional nature, in a sense that the standard BCS theory

employing phonon-mediated Cooper pair formation [4] cannot be applied.

Superconductivity existing near a (putative) QCP naturally implies its close proximity to magnetic order within the phase diagram. While in classical superconductors these two many-body quantum phenomena are caused by different (itinerant and localized) species of electrons and are mutually exclusive, in the heavy fermion metals the hybridized *f* electrons, often called composite fermions, are not only responsible for the magnetic order, but are also carrying the superconductivity. Consequently, magnetism and superconductivity may not only compete but may even coexist in these systems. *Microscopic coexistence* of superconductivity and magnetic order both involving the *same* charge carriers is an especially striking example for complex behavior of emerging materials exhibiting intertwined ground states.

In this context the CeMIn₅ family of heavy-fermion compounds offers an interesting playground [5]. The intricate interplay of superconductivity and magnetism is, *e.g.*, manifested by the existence of superconductivity found in CeCoIn₅ below $T_c \approx 2.3$ K and antiferromagnetic order in CeRhIn₅ below $T_N \approx 3.7$ K. Conversely, superconductivity is observed in the latter compound by the application of pressure [6] whereas neutron scattering experiments indicate strong antiferromagnetic quasielastic excitations in the paramagnetic regime of CeCoIn₅ [7]. Moreover, the existence of a field-induced QCP has been anticipated [8,9].

Here, we summarize our progress towards deeper insight into the interplay of unconventional superconductivity and quantum criticality in CeCoIn₅, CeIrIn₅ and Cd-substituted CeCo(In_{1-x}Cd_x)₅. High precision structural investigations indicate the existence of a certain type of point defect in the tetragonal HoCoGa₅ structure that might well influence the material's physical properties. These defects are inferred from enhanced resolution X-ray diffraction experiments and can directly be visualized by Scanning Tunneling Microscopy (STM). Earlier

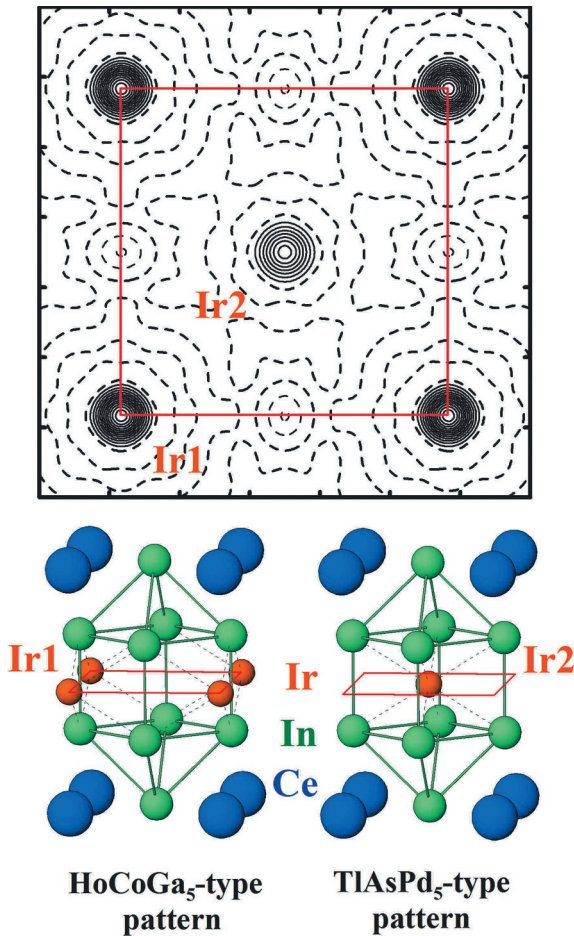


Fig. 1: Two closely related structure types HoCoGa_5 (bottom left) and TlAsPd_5 (bottom right) and the superposition of their structural patterns in the crystal structure of CeIrIn_5 . The presence of about 1% of Ir in Ir2 positions (TlAsPd_5 pattern) at $z = 0.5$ is indicated (top) by the difference electron density calculated from enhanced-resolution X-ray diffraction experiments on our single crystals of CeIrIn_5 (see text).

findings of a precursor state to superconductivity in CeCoIn_5 [10] and CeIrIn_5 [11] (reminiscent of the *pseudogap* observed in the cuprates) are confirmed by our Scanning Tunneling Spectroscopy (STS). Finally, we report on the duality of the electronic $4f$ degrees of freedom which can be more or less localized for different parts of the Fermi surface [12].

Structural investigations

Normal-resolution X-ray diffraction experiments (MoK α radiation, $2\theta_{\text{max}} = 52.62^\circ$, 131 reflections, $R(F) = 0.052$ [13]) indicated that CeIrIn_5 crystallizes in the structure type HoCoGa_5 [14]. However,

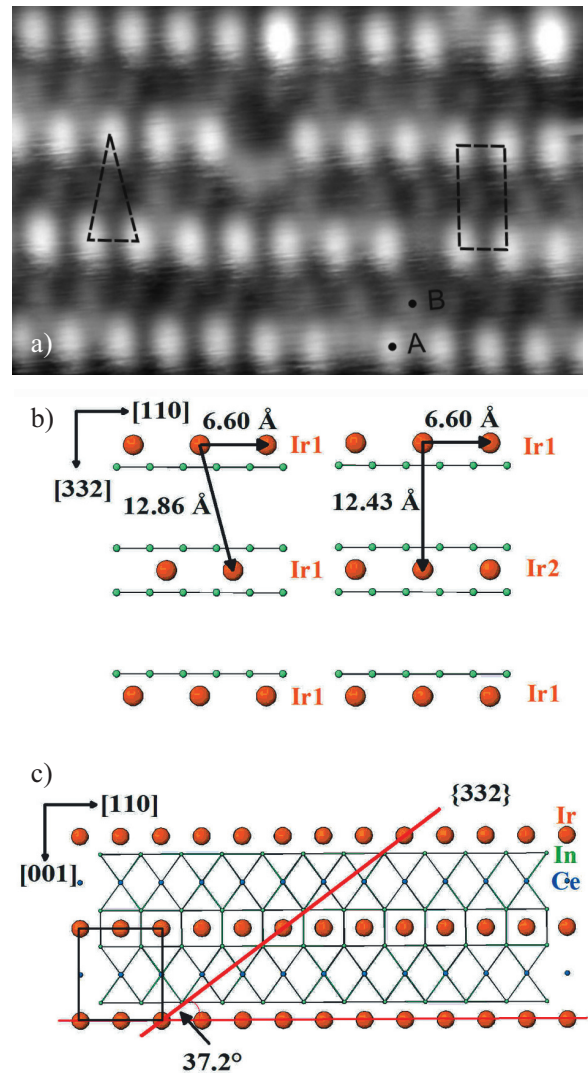


Fig. 2: (a) STM topography on a CeIrIn_5 surface obtained by in situ cleaving. The image covers an area of $5.0 \text{ nm} \times 7.7 \text{ nm}$ and a height scale of 0.63 nm . Markers A and B indicate two kinds of atomic corrugations whereas the dashed rectangle and triangle illustrate atoms of type A in different arrangements. $V = 600 \text{ mV}$, $I_{\text{set}} = 0.3 \text{ nA}$, $T = 330 \text{ mK}$.

(b) Arrangement of the Ir and In atoms in the $\{332\}$ plane of the HoCoGa_5 (left) and the TlAsPd_5 structure (right). (c) Visualization of the $\{332\}$ plane and its inclination angle with respect to the (001) plane.

the results of the STM topography studies discussed below insinuated a more complex structure, at least at the sample surface. In an effort to possibly relate surface and bulk structural properties, we performed an enhanced diffraction experiment (space group $P4/mmm$, $a = 4.6660(3) \text{ \AA}$, $c = 7.5161(7) \text{ \AA}$, MoK α radiation, $2\theta_{\text{max}} = 70.35^\circ$, 240 reflections, $R(F) = 0.020$). The distribution of the difference electron density in the plane at

$z = 0.5$ calculated from these diffraction experiments and without iridium atoms (Fig. 1, top) exhibits maxima at the edges of the unit cell (position Ir1) which are expected for the structural pattern of the HoCoGa₅ type (Fig. 1, bottom left). In addition, however, maxima of the difference electron density were also found in the center of the unit cell (position Ir2), which is characteristic for the structure pattern of TlAsPd₅ type (Fig. 1, bottom right [15]). Final refinement resulted in occupancies of $occ(\text{Ir1})=0.988$ and $occ(\text{Ir2})=0.012$. Consequently, the crystal structure of the investigated crystals of CeIrIn₅ reveals a non-negligible disorder of the Ir atoms. The presence of Ir atoms at two different positions is a key observation for understanding the atomic distribution on the surface as seen in the STM experiments.

In an attempt to directly visualize the crystal structure as well as the disorder discussed above we conducted STM. Because STM is a particularly surface sensitive technique special attention has to be paid with respect to the sample surface quality. Therefore, the STM utilized here is operated in UHV ($p \leq 2 \times 10^{-9}$ Pa) and equipped for *in situ* sample cleaving [16]. Moreover, sample temperatures as low as 0.32 K can be obtained which is of importance for the investigation of superconductivity in CeCoIn₅ by STS (see below) as well as for providing an adequate energy resolution (≤ 100 μeV , as verified by investigating the superconducting energy gap of Al).

Atomically resolved images of CeMIn₅ were obtained on areas of up to 60 nm \times 60 nm, exhibiting terraces of various lattice planes with up to a few ten nm in extent. Figure 2(a) exemplifies such a terrace of atomically resolved topography on CeIrIn₅. The sample had been mounted parallel to the crystallographic *ab*-plane. A high tilting angle of the imaged sample area of 37° with respect to the scanning plane points towards a plane of low symmetry. This slope has been taken into consideration when calculating the interatomic distances. We suggest that the terminating surface is a {332} plane for which an inclination of 37.2° is expected, *cf.* Figure 2(c). Moreover, within this plane the adjacent Ir atoms should be spaced by 6.6 Å, Figure 2(b). The distances of the A-type atoms within the lines observed in STM topography, (6.7 \pm 0.3) Å, are in reasonable agreement with the shortest distances between the Ir atoms within the {332} plane of CeIrIn₅. Here we should note that

for positive bias voltage as applied in Figure 2(a) the Ir atoms should appear as the brightest entities since they accumulate the strongest negative charge. Therefore, the most prominent corrugations marked by A in Figure 2(a) are very likely Ir atoms. The corrugations marked as B could then originate from the In atoms of the intermediate In layers as shown in Figures 2(b) and (c). For position B the assignment to a certain atomic species is somewhat hindered because, in addition to the actual height, also a changed density of states (DOS) may affect the apparent height.

The analysis of the arrangements of Ir atoms in the {332} plane of the HoCoGa₅ and the TlAsPd₅ structure type reveals two different possibilities, see Figure 2(b). If only Ir1 atoms are present in the structural pattern, the local configuration of Ir atoms in the {332} plane exhibits a typical triangular network, Figure 2(b) left, an arrangement that is indeed very often observed in the STM images, Figure 2(a). If iridium atoms are located also in the Ir2 positions, Figure 2(b) right, then the atomic arrangement of Ir in the {332} plane exhibits a rectangular pattern, which is rarely but nonetheless found in the experiment. In addition, the observed distances between the lines of corrugations of type A are (13.7 \pm 0.8) Å, which is only slightly larger than the expected spacing between the Ir lines measured in [332] direction.

Consequently, our STM topography directly confirms the existence of defects as indicated by the structural refinement. Unfortunately, our STM topography does not allow for a statistical analysis to estimate the amount of Ir occupying such defective positions. In addition, the cleaving might take place along planes of increased defect density which may render a quantitative comparison between the X-ray and STM results difficult.

Spectroscopy of the superconducting state

Our magnetotransport investigations on the system CeIrIn₅ indicated the existence of a precursor state to superconductivity [11]. The analysis that led to such an inference relied on the so called Hall angle $\theta_{\text{H}} = \cot^{-1}(\rho_{\text{xx}} / \rho_{\text{xy}})$, *i.e.* on the ratio of magneto- and Hall resistance. In particular, it was demonstrated that the modified Kohler's scaling – relating the magnetoresistance to the Hall angle – breaks down prior to the onset of superconductivity

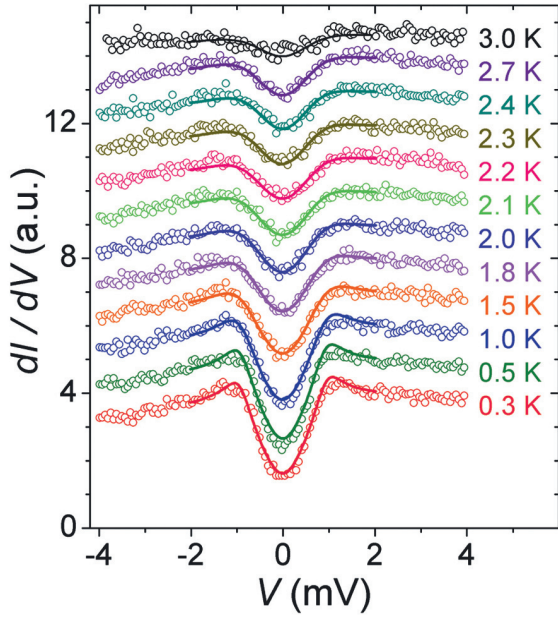


Fig. 3: Differential conductance obtained by Scanning Tunneling Spectroscopy on CeCoIn₅ (open circles) at several temperatures. The persistence of a gap-like behavior above $T_c \approx 2.3$ K is clearly visible. The lines represent fits according to BCS theory (see text). For clarity, the curves are offset vertically.

due to a change in the Hall scattering rate [17]. Moreover, it could be shown that the Hall coefficient R_H and ρ_{xx} are governed by two distinct scattering times [18]. It should be emphasized that both observations – a pseudogap-like precursor state and the existence of two distinct scattering times – are highly reminiscent of the behavior found for the copper oxide superconductors. All these observations are also consistent with a scenario in which incipient antiferromagnetic fluctuations crucially influence the magnetotransport in both classes of materials, the fermion systems as well as the cuprates.

In case of the cuprate superconductors, STS has proven to be a powerful tool for the investigation of the superconducting gap and, specifically, of the pseudogap [19]. Therefore, we attempted STS on single crystalline CeMIn₅ ($M = \text{Co, Ir}$) compounds. We emphasize that STS provides direct information about the electronic DOS of the sample. In order to prepare clean surfaces a stainless steel post was glued onto the ab -plane of the samples and torn off *in situ*. In addition, we regularly checked on the quality of the tunnel junctions by measuring the current dependence on tip-sample distance, $I(z)$, from the slope of which the work function Φ can be determined. Only junctions with $\Phi \geq 2$ eV were investigated further.

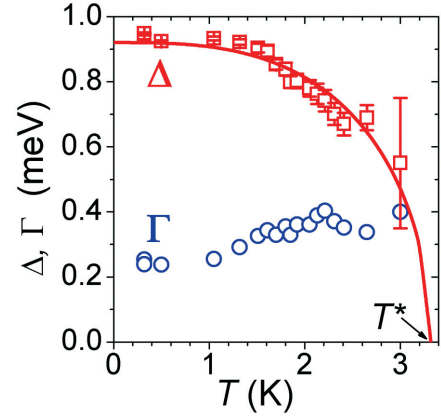


Fig. 4: Gap energy $\Delta(T)$ and lifetime broadening parameter $\Gamma(T)$ as obtained from fitting the conductance spectra at each measured temperature. The solid line is a fit to eq. (2).

In Figure 3, differential conductance (dI/dV^{-1}) spectra are presented as obtained for CeCoIn₅ within atomically flat terraces and within a temperature range $0.32 \text{ K} \leq T \leq 3 \text{ K}$. The curves were acquired with a bias voltage of $V = 14 \text{ mV}$ at a set-point current of $I_{\text{set}} = 340 \text{ pA}$ and are shifted vertically (except the one obtained at $T = 0.32 \text{ K}$) for clarity. Upon increasing temperature the zero bias conductance increases, indicating a closing of the gap. The gap, however, does not disappear at $T_c \approx 2.3 \text{ K}$, but is still clearly visible at $T = 3 \text{ K}$.

For an analysis of our conductance spectra [20], we assumed a superconducting order parameter of $d_{x^2-y^2}$ symmetry as suggested in the literature [21,22]. In this case, the BCS expression for the superconducting excitation spectrum takes the form [23]

$$\rho(E) \propto \text{Re} \int_0^{2\pi} \frac{d\phi}{2\pi} \frac{E - i\Gamma}{\sqrt{(E - i\Gamma)^2 - \Delta^2 \cos^2(2\phi)}} \quad (1)$$

where Δ is the maximum value of the angular dependent gap function. The additional lifetime broadening parameter Γ accounts for in-gap states due to inelastic scattering [24]. Fits of eq. (1) to our conductance spectra are included in Figure 3 (lines) and yielded Δ and Γ for each T measured. The latter are presented in Figure 4. Expectedly, the superconducting order parameter $\Delta(T)$ decreases with temperature, whereas $\Gamma(T)$ slightly increases. For nodal superconductors it is expected [25] that

$$\Delta(T) = \Delta_0 \sqrt{1 - (T/T^*)^3} \quad (2)$$

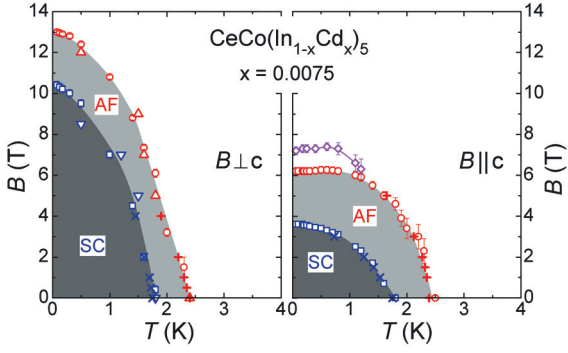


Fig. 5: Magnetic field – temperature phase diagram for $\text{CeCo}(\text{In}_{0.9925}\text{Cd}_{0.0075})_5$ with B applied perpendicular (left) and parallel (right) to the crystallographic c axis. Data represent results of magnetotransport (\circ, \square), neutron scattering (Δ, ∇) and heat capacity ($+, \times$) measurements indicating the antiferromagnetic (AF, red) and superconducting (SC, blue) transition.

where T^* denotes the temperature at which $\Delta(T)$ extrapolates to zero. Fitting our values $\Delta(T)$ to eq. (2) yields $T^* \approx 3.3$ K which is clearly beyond $T_c \approx 2.3$ K. Yet, given the extreme surface sensitivity of STS this result should be compared to other, preferably bulk measurements. Indeed, early measurements of the electrical resistivity under pressure indicated the opening of a pseudogap below 3.3 K at ambient pressure [10]. We also note that thermal conductivity [21] and neutron scattering experiments [7] suggested that remnants of the superconducting state prevail beyond T_c . All these results support our conjecture of the existence of a precursor state to superconductivity in the CeMIn_5 compounds.

The interplay between magnetic and superconducting order in the 115 family of compounds becomes immediately apparent if Cd substituted $\text{CeCo}(\text{In}_{1-x}\text{Cd}_x)_5$ is studied. With increasing Cd content x , T_c is suppressed whereas the antiferromagnetic order is stabilized [26]. In the following we focus our investigation on the specific composition $x = 0.0075$ since here, $T_c \approx 1.7$ K and the antiferromagnetic ordering temperature $T_N \approx 2.4$ K are closest within this series and hence, the involved energy scales are expected to be comparable. Measurements of magnetotransport, neutron scattering and heat capacity were conducted on samples of the same batch or, where possible, on the very same sample in an effort to unambiguously identify the signatures of the two ordering phenomena. Indeed, the excellent agreement of the results (Fig. 5) verifies that bulk properties are

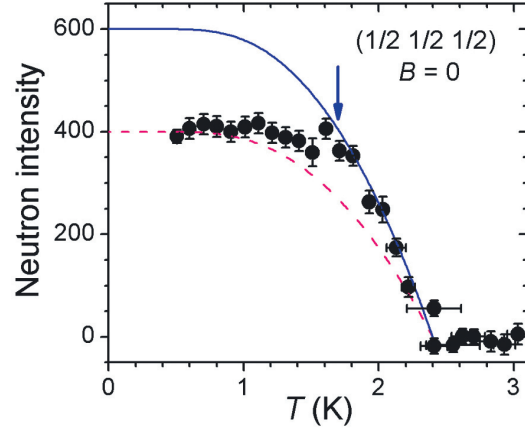


Fig. 6: Temperature dependence of magnetic intensity in $\text{CeCo}(\text{In}_{0.9925}\text{Cd}_{0.0075})_5$ obtained by elastic neutron scattering scans along [001] and at $(\frac{1}{2} \frac{1}{2} \frac{1}{2})$ for zero magnetic field. The lines represent mean-field expectations to the data (see text). For the blue line only the temperature range $T_c < T < T_N$ was considered. Blue arrow indicates T_c .

probed for all three methods. The strikingly equivalent behavior of the superconducting and antiferromagnetic phase boundary, in particular for magnetic field $B \perp c$, is indicative of a mutual influence of the two phenomena. The steep initial slope of $T_c(B)$ of approximately $-13(-4)$ T/K for $B \perp(\parallel) c$ indicates a large effective quasiparticle mass, *i.e.* heavy fermion superconductivity.

To gain further insight into a possible interplay between superconductivity and antiferromagnetic order, the magnetic intensity in elastic neutron scattering at $(\frac{1}{2} \frac{1}{2} \frac{1}{2})$ was recorded as a function of temperature for different magnetic fields [12]. In zero magnetic field, Figure 6, the magnetic intensity increases below T_N and displays a kink at T_c (marked by the blue arrow) with no further change in intensity at lower temperatures. The assignment of this kink to T_c is corroborated by the magnetotransport and heat capacity measurements. An attempt to fit the zero-field magnetic intensity by a mean-field model for the sublattice magnetization (using a Brillouin function for an effective spin- $\frac{1}{2}$ system) fails to describe the whole temperature dependence, as indicated by the dashed magenta line in Figure 6. However, a fit restricted only to the temperature range $T_c < T < T_N$ reproduces these data reasonably well (solid blue line in Fig. 6). This fit results in an expected magnetic intensity for $T \rightarrow 0$ of about 40% larger than the experimentally observed saturation value. Obviously, the onset of superconductivity prevents a further rise of mag-

netic intensity below T_c without suppressing the antiferromagnetic order itself. Very similar behavior of the magnetic intensity was observed for applied magnetic field, with accordingly reduced values of T_N , T_c and overall magnetic intensity.

The almost constant neutron intensity below T_c is intriguing. Our analysis [12] indicates a second order phase transition at T_c without spatial phase separation. Then, the deviation of the neutron intensity from its expected value below T_c implies coexistence and, more importantly, mutual influence of antiferromagnetic and superconducting order which are correlated via identical $4f$ states. We speculate that the low-energy magnetic fluctuations are gapped by superconductivity and likely shifted to higher energies (possibly to a resonance similar to the one observed at 0.6 meV in undoped CeCoIn₅ [7]), a similar mechanism as discussed for the cuprates [27]. The delicate, unprecedented balance of the two states may result from the proximity of T_c and T_N in the chosen compound.

Summary

The combination of enhanced-resolution X-ray investigations and STM topography on identical single crystals of CeIrIn₅ provided unprecedented structural insight: Beside the expected HoCoGa₅ structural pattern also the presence of about 1% of Ir in Ir2 positions (belonging to the TlAsPd₅ pattern) at $z = 0.5$ was indicated by both types of measurement. Further, Scanning Tunneling Spectroscopy revealed the superconducting gap to persist up to about 3.3 K, *i.e.* beyond $T_c \approx 2.3$ K, in reminiscence of the pseudogap observed in the cuprate superconductors. An extraordinary coexistence and mutual influence of the superconducting and antiferromagnetic order in slightly Cd-doped CeCoIn₅ was inferred.

References

- [1] *S. Doniach*, Physica B **91** (1977) 231.
- [2] *N. D. Mathur et al.*, Nature **394** (1998) 39.
- [3] *D. M. Broun*, Nature Phys. **4** (2008) 171.
- [4] *J. Bardeen, L. N. Cooper and J. R. Schrieffer*, Phys. Rev. **108** (1957) 1175.
- [5] *J. L. Sarrao and J. D. Thompson*, J. Phys. Soc. Jpn. **76** (2007) 051013.
- [6] *T. Park et al.*, Nature **456** (2008) 366.
- [7] *C. Stock et al.*, Phys. Rev. Lett. **100** (2008) 087001.
- [8] *J. Paglione et al.*, Phys. Rev. Lett. **91** (2003) 246405.
- [9] *A. Bianchi et al.*, Phys. Rev. Lett. **91** (2003) 257001.
- [10] *V. A. Sidorov et al.*, Phys. Rev. Lett. **89** (2002) 157004.
- [11] *S. Nair et al.*, Phys. Rev. Lett. **100** (2008) 137003.
- [12] *S. Nair et al.*, Proc. Natl. Acad. Sci. USA **107** (2010) 9537.
- [13] *E. G. Moshopoulou, Z. Fisk, J. L. Sarrao, and J. D. Thompson*, J. Solid State Chem. **158** (2001) 25.
- [14] *Yu. Grin, Ya. P. Yarmolyuk, E. I. Gladyshevski*, Sov. Phys. Crystallogr. **24** (1979) 137.
- [15] *M. El-Boragy and K. Schubert*, Z. Metallkd. **61** (1970) 579.
- [16] *S. Wirth, A. Bettac, S. Ernst, A. Gladun, M. Rams, and F. Steglich*, in Scientific Report 2003-2005, p. 51 (Max Planck Institute for Chemical Physics of Solids, Dresden Germany, 2006).
- [17] *S. Nair et al.*, Phys. Rev. B **79** (2009) 094501.
- [18] *S. Nair et al.*, J. Supercond. Nov. Magn. **22** (2009) 201.
- [19] *Ø. Fischer, M. Kugler, I. Maggio-Aprile, C. Berthod, and C. Renner*, Rev. Mod. Phys. **79** (2007) 353.
- [20] *S. Ernst et al.*, Phys. Status Solidi B **240** (2010) 624.
- [21] *K. Izawa, H. Yamaguchi, Y. Matsuda, H. Shishido, R. Settai, and Y. Ōnuki*, Phys. Rev. Lett. **87** (2001) 057002.
- [22] *A. Vorontsov and I. Vekhter*, Phys. Rev. Lett. **96** (2006) 237001.
- [23] *H. Won and K. Maki*, Phys. Rev. B **49** (1994) 1397.
- [24] *R. C. Dynes, V. Narayanamurti, and J. P. Garno*, Phys. Rev. Lett. **41** (1978) 1509.
- [25] *B. Dóra and A. Virosztek*, Eur. Phys. J. B **22** (2001) 167.
- [26] *L. D. Pham, T. Park, S. Maquilon, J. D. Thompson, and Z. Fisk*, Phys. Rev. Lett. **97** (2006) 056404.
- [27] *T. Dahm et al.*, Nature Phys. **5** (2009) 217.

¹Département de Physique, Université de Montréal, Montréal, Quebec H3C 3J7, Canada

²University of California, Irvine, California 92697, USA

³Present address: Indian Institute of Science, Education and Research (IISER), Dr Homi Bhabha Road, Pune 411008, India

⁴Los Alamos National Laboratory, Los Alamos, New Mexico 87545, USA

⁵Institut für Festkörperphysik, TU Dresden, 01062 Dresden und Helmholtz-Zentrum Berlin für Materialien und Energie, 14109 Berlin, Germany